



An approach to predict soil salinity changes in irrigated pistachio orchards (Ardakan, Yazd Province): A case study

Somayeh Shamsi¹, Ardavan Kamali^{2†} and Yousef Hasheminejad³

¹ Grad. Student and ² Associate Professor, College of Agriculture, Vali-e-Asr University of Rafsanjan, Rafsanjan, 771889711, Iran

³ Assistant Professor, National Salinity Research Center (NSRC, AREEO), Yazd, 8917357676, Iran

†Corresponding Author Email: A.kamali@vru.ac.ir

(Received 2021/13/11, Accepted 2022/27/04)

ABSTRACT

The sustainability production of dryland agriculture is threatened by salt accumulation in soil due to irrigation practices by saline waters. However, the dynamic processes of secondary soil salinization depend on some factors varying in time and space. The aim of this research was to introduce an approach for the prediction of soil salinity in some irrigated pistachio (*Pistacia vera* L.) orchards facing secondary soil salinization. The study area was Ardakan (Yazd Province, Central Iran). In this approach, the Landsat 8 satellite data bands and satellite-based driven data (indices) were used. The Partial Least Square Regression (PLSR) method was used to predict the variability of soil salinity with minimum (zero) ground measurements. The predicted soil salinity (electrical conductivity) of soil saturated paste extract (EC_e) were compared by the measured EC_e . The existing conventional methods (e.g. WatSuit computation model) using ancillary measured data of irrigation water salinity (EC_{iw}) and corresponding leaching fractions (LF) were also used for evaluation. The Results of the satellite-based PLSR method showed an R^2 of about 64% between predicted and measured soil salinity, while this indicator was about 72% for the conventional model of WatSuit. The higher accuracy of the Watsuit model is owing to its dependence on ground measurements, while the introduced satellite-based PLSR approach was able to predict temporal changes of soil salinity in patterns fitted to the irrigation intervals with zero dependence on the ground truth data.

Keywords: Irrigation, Modeling, Salinity, Spectral indices, WatSuit.

1. Introduction

Salinization is the dominant soil degrading process in arid lands and has an adverse effect on soil quality attributes and agricultural productivity (Moharana et al., 2019). Soil salinization can be formed as a result of two major types of processes that may occur simultaneously. Natural (primary) soil salinization is dominant in virgin lands of arid regions which are rich in salts in their parent materials or due to the shallow groundwater tables. Other natural agents such as salt intrusion from seas and weathering may also develop primary soil salinization. Anthropogenic (secondary) soil salinization is a human-induced process, mainly as a result of irrigation with saline water or poor irrigation and drainage management (Cheraghi et al., 2008). Globally, about 30 percent of irrigated lands are estimated to be affected by secondary soil salinization. This value is expected to touch more than 50 percent of the irrigated lands in Iran (Qadir et al., 2008). The global economic impacts of soil salinization due to crop yield loss are estimated from 12 (Ghassemi et al., 1995) to 27.3 billion USD (Qadir et al., 2014), while for the State of California alone it touches 3.7 billion USD (Welle and Mauter, 2017).

The central Iranian plateau, with less than 50 mm annual precipitation, constitutes the hottest and driest part

of the country where agriculture is dependent on the deep aquifers of pumped groundwater, with the salt content of more than 1.5 g/L in most cases (Cheraghi et al., 2007). Salinity-tolerant crops, such as cotton, wheat, barley, sugar beet, and pistachio, are the main constituents of cropping patterns in the region. The salinity of groundwater has risen as a result of the overdraft, and there is a tendency to grow more salinity-tolerant crops (e.g., pistachio) using marginal quality water. The salinity of irrigation water reaches 20 dS/m in some irrigated pistachio orchards.

There is a rising concern among the farmers and local decision-makers about the fate of solutes added to the soil within (Hasheminejad et al., 2012) and beneath (Hasheminejad et al., 2012) the root zone. Soil salinity could therefore threaten the sustainability of production systems.

Long-term spatial variations of soil salinity in irrigated farms are a function of irrigation water salinity and leaching fraction (Manzoor et al., 2019), a fraction added to irrigation requirement to leach the salts below the root zone. Leaching fraction, in turn, is a function of evaporation demand, irrigation depth, crop growth stage, and its performance, which can change soil salinity in short term (Baghzouz et al., 2006). Steady-state models have been developed to predict long-term variations of

soil salinity, while transient state models consider short-term variations under inhomogeneous soil and management conditions (Corwin et al., 2007).

The extent of salinity buildup in irrigated fields is dependent on the number of solutes leached beneath the root zone (Manzoor et al., 2019). Water Suitability (WatSuit) is a steady-state model (Rhoades et al., 1992) that considers the effects of irrigation water chemical composition and leaching fraction on soil salinity under the assumption of a trapezoidal pattern of water extraction by sequential quarters of the root zone. While steady-state models, such as WatSuit, depend on general data (Alexandre et al., 2018) for their simulations, transient state models require extended and detailed information about the whole system of production and in turn, provide detailed outputs. The models are also able to predict soil salinization and sodification with the least dependence on the ground truth data (Alexandre et al., 2018).

However, it is difficult to provide this steady state model for large-scale and transient state conditions (Corwin and Grattan, 2018). In this context, another modeling approach could facilitate the time, labor, and costs of monitoring and preparing of the required data. In this approach, satellite remote sensing images (Mandal, 2019) can be used as a source of input data as well as to provide an opportunity to scale out results of the modeling with the lowest cost (Metternicht and Zinck, 2003). Moreover, interpolation of sizeable data in combination with Google Earth Engine (GEE) also can be used to produce the global map of soil salinity changes (Ivushkin et al., 2019). The aim of this study is to introduce an approach for prediction of soil salinity for irrigated lands, facing with transient conditions of secondary soil salinization process. In this approach, Landsat 8 satellite data bands and satellite-based driven data (indices) along with multiple regression method have been used to explain variability of the soil salinity with minimum (zero) ground measurements. This approach has been compared with the Watsuit (Oster and Rhoades 1990) results and evaluated using the measured soil salinity data, as well.

2. Materials and Methods

2.1. Study area

The study area includes pistachio orchards spread in about 4000 ha as green patches in North Ardakan (32° 18'N and 53° 50'E), Yazd province, Iran (Fig. 1). Pistachio orchards are irrigated with groundwater pumped from a depth of more than 60 meters. A total of 134 wells and Qanats are now being exploited with salinities of about 2.5-20.0 dS/m with an average of 10.91 dS/m. Each well is shared among a group of farmers, which makes the management and farm conditions quite different between individual fields. Owing to the salinity tolerance of pistachio trees, only 30

wells have salinities lower than the threshold and almost all orchards suffer from different levels of salinity stress. Improper irrigation management has also led to soil salinization as a result of salinity buildup in the root zone.

2.2. Ground-based data of salinity

Soil salinity in irrigated fields is in equilibrium with irrigation water salinity (Minhas et al., 2020). In this study, we used the pre-defined chemical analysis of 134 well water sources to determine the proper sampling density and locations. These data which included EC and ion composition were interpolated over the study area to convert point values to raster. These data, along with some vegetation indices derived from Landsat 8 images (Jin et al., 2018), were used as auxiliary data in conditioned Latin hypercube sampling strategy (Minasny and McBratney 2006) to determine sampling points. Ground data have been acquired from 18 representative points scattered across the study area. These points are shown by green dots in Fig. 1. Each point consists of a pistachio orchard, irrigated with a water source (deep well), covering an area of about 15 to 60 ha. Chemical compositions of the irrigation waters in the sampling points have been illustrated in Table 1. Considering the salinity tolerance threshold of pistachio as 8 dS/m, these irrigation water sources are in a non-saline to highly-saline range. Regarding the sodicity, the SAR value varies in the range of about 9.5 (non- sodic) to 27 (highly-sodic). The same is true about alkalinity (bicarbonate concentration) with a range of less than 2 to more than 6 meq/L.

Soil of each point (orchard) was sampled down to a depth of 90 cm at 30 cm increments. Samples were analyzed in a laboratory, concerning salinity levels and concentrations of soluble ions in the soil saturated paste extract. The leaching fraction (LF) is an essential variable to predict soil salinity of the irrigated lands, while it cannot be measured easily in the areas like Ardakan pistachio orchards, where the drainage water is not accessible under deep free drainage conditions. In this case, the LF was determined through dividing the EC of the irrigation water (EC_{iw}) by the EC of the drainage water (EC_{dw}), collected by installing a modified version of a funnel-shaped wetting front detector (WFD) device (Rahimian et al., 2019) at 90 cm depth from the soil surface in each sampling point. The WFD is a simple device, first was introduced for irrigation scheduling (Stirzaker, 2003), and permits access to a sample of drainage water (Stirzaker, 2005), which could be used to calculate LF under the actual field conditions (Hasheminejhad 2011). Figure 2 shows scheme of the prepared modified WFD for measuring LF values in the representative orchards.

Moreover, the WatSuit model (Oster and Rhoades, 1990), as a conventional method for prediction of soil salinity was used in this study. The model requires the

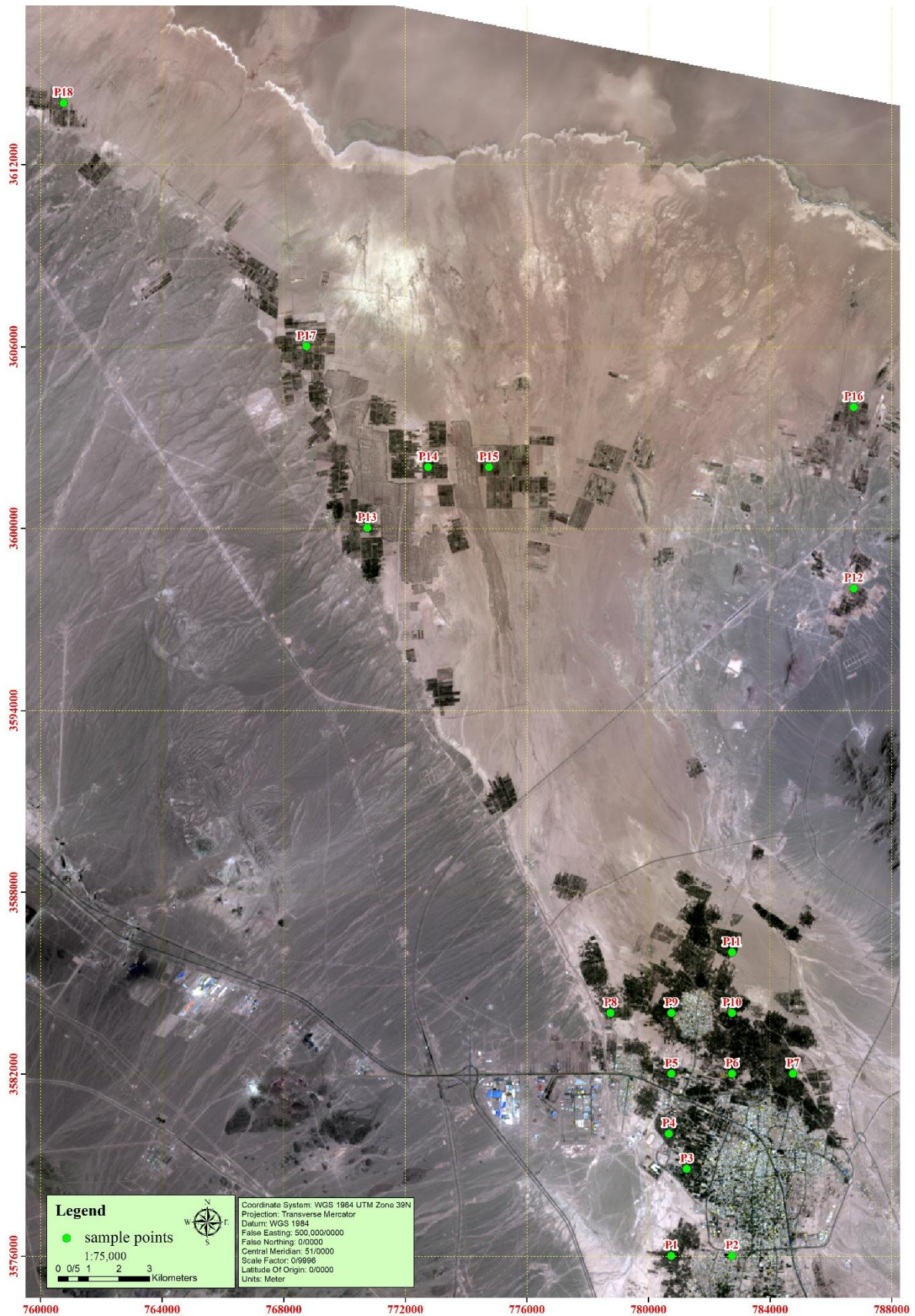


Fig. 1. The extent of the study area and sampling points in North Ardakan, Yazd Province, Iran

Table 1. The chemical compositions of irrigation water in the sampling points

Points	EC _{iw}	Ca ²⁺	Mg ²⁺	Na ⁺	K ⁺	Cl ⁻	HCO ₃ ⁻	SO ₄ ²⁻	SAR
	dS/m	meq/L							(meq/L) ^{-1/2}
P1	3.93	4.17	7.29	26.94	0.42	17.97	5.45	15.40	11.25
P2	4.00	4.30	7.42	27.43	0.43	18.64	5.43	15.51	11.33
P3	4.12	5.74	9.12	25.93	0.33	24.32	6.51	10.29	9.51
P4	3.81	4.78	7.36	23.52	0.38	20.90	5.67	9.47	9.55
P5	3.93	4.83	7.86	25.73	0.33	22.63	4.60	11.52	10.21
P6	10.53	11.24	22.68	76.17	0.66	82.77	2.95	25.03	18.50
P7	10.07	12.59	11.42	76.17	0.36	81.45	1.80	17.29	21.98
P8	9.65	19.07	30.71	56.18	0.86	66.34	6.62	33.86	11.26
P9	12.70	10.67	22.57	99.13	0.60	98.10	4.73	30.14	24.32
P10	17.39	27.70	43.29	117.39	0.73	151.66	3.72	33.73	19.70
P11	14.39	16.22	21.37	118.04	0.48	115.26	3.02	37.83	27.23
P12	14.32	28.11	22.36	108.39	0.31	104.67	2.01	52.49	21.58
P13	11.21	23.39	20.93	76.26	0.86	79.36	4.50	37.58	16.20
P14	8.96	13.34	12.64	68.37	0.83	65.24	5.91	24.03	18.97
P15	19.14	27.15	30.91	138.69	1.60	164.90	5.86	27.59	25.74
P16	16.48	26.62	23.07	110.60	0.39	148.40	1.98	10.30	22.19
P17	11.11	22.61	18.79	74.28	0.88	83.88	5.30	27.38	16.33
P18	19.44	45.96	44.32	128.56	0.52	175.90	2.43	41.03	19.13

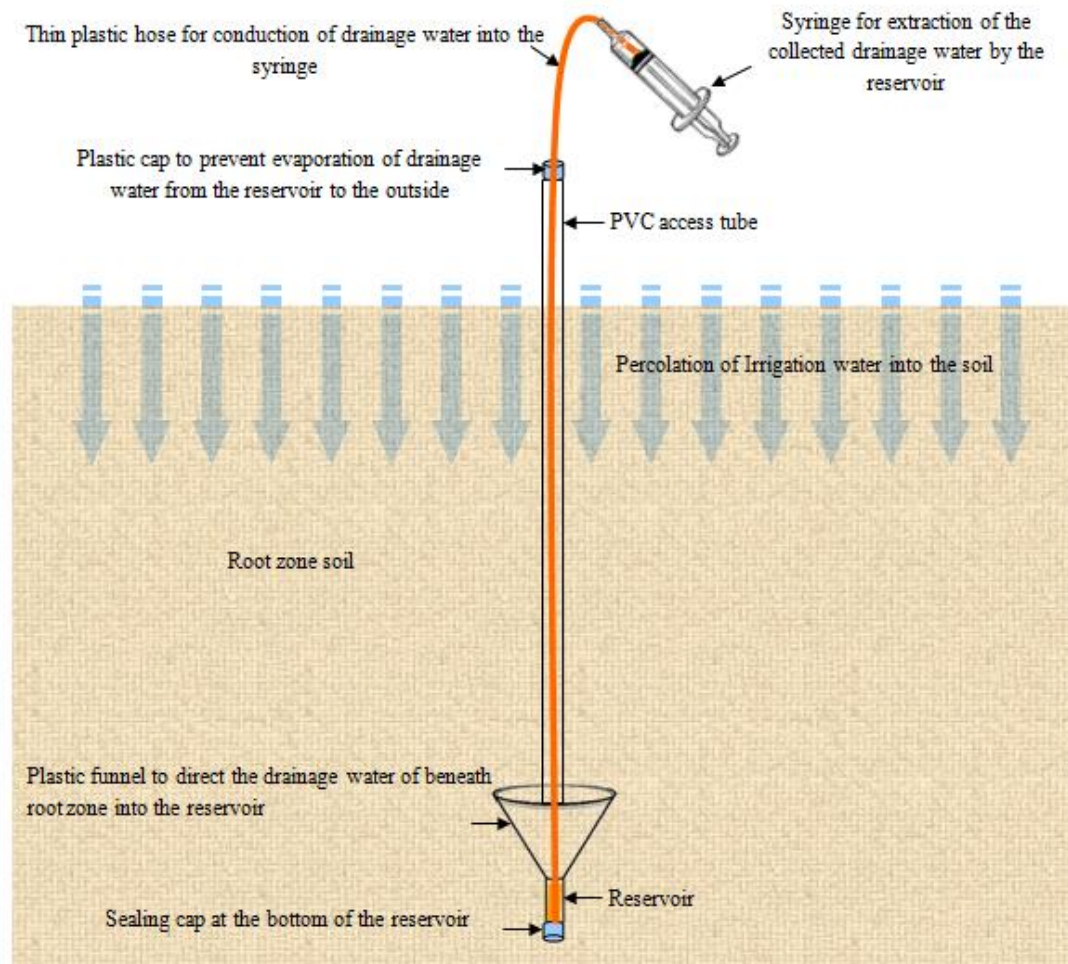


Fig. 2. A modified version of Wetting Front Detector device (Rahimian et al., 2019 originally from Stirzaker, 2003), for extraction of the root zone drainage water, measurement of its electrical conductivity (EC_{dw}) and calculation of the leaching fraction (LF) in the pistachio irrigated orchards

Table 2. The spectral indices extracted from Landsat eight (OLI) images

Index	Formula	Reference
Normalized Difference Vegetation Index (NDVI)	$\frac{(\text{Band5} - \text{Band4})}{(\text{Band5} + \text{Band4})}$	(Vermote et al., 2016)
Soil Adjusted Vegetation Index (SAVI)	$\frac{(\text{Band5} - \text{Band4})}{(\text{Band5} + \text{Band4} + 0.5)} \times 1.5$	(Vermote et al., 2016)
Normalized Difference Salinity Index (NDSI)	$\frac{(\text{Band4} - \text{Band5})}{(\text{Band4} + \text{Band5})}$	(Noroozi et al., 2011)
Leaf Area Index (LAI)	$21.202 \times \text{SAVI}^2 - 2.905 \times \text{SAVI} + 2.948$	(Mokhtari et al., 2013)
Normalized Burned Ratio Index (NBRI)	$\frac{(\text{Band5} - \text{Band7})}{(\text{Band5} + \text{Band7})}$	(Vermote et al., 2016)
Bare Soil Index (BSI)	$\frac{(\text{Band6} + \text{Band4}) - (\text{Band5} + \text{Band2})}{(\text{Band6} + \text{Band4}) + (\text{Band5} + \text{Band2})}$	(Vermote et al., 2016)

chemical compositions of the irrigation water (Table 1) and the leaching fraction (LF) as the main input parameters. As mentioned before, the LF values were calculated using Equation (2) and based on the results of the WFD device.

With the assumptions of steady-state salt and water balance, the product of irrigation water salinity (EC_{iw}) and its volume (V_{iw}) is equal to that of drainage water salinity (EC_{dw}) and its volume (V_{dw}):

$$EC_{iw} \times V_{iw} = EC_{dw} \times V_{dw} \quad [1]$$

Rearrangement of Equation 1 leads to the definition of the leaching fraction (LF) as Equation 2:

$$LF = \frac{V_{dw}}{V_{iw}} = \frac{EC_{iw}}{EC_{dw}} \quad [2]$$

The latter form presents two terms for LF definition: in terms of water (LF_w) and salinity (LF_{EC}). Long-term simulation of salinity in almond orchards (Yang et al., 2019) showed that these two terms could be equal after about 10 years. Assuming the 40-30-20-10 rule of thumb for the extraction of water from sequential root zone quarters, (Ayers and Westcot, 1985) presented an LF-dependent concentration factor (X) for the calculation of mean root zone salinity:

$$\overline{EC_e} = X \cdot EC_{iw} \quad [3]$$

Further evaluations showed that the actual soil salinity could be considerably lower than the value predicted by Equation (3) due to the precipitation of some minerals, especially at lower LF values.

2.3. Satellite-based prediction of soil salinity

Satellite data were retrieved from Landsat 8 satellite images of 2019. Cloud-free images of May 14th, and 30th, Jun 15th, July the 1st, and 17th, August 2nd, and 18th were downloaded from <https://earthexplorer.usgs.gov/>, and the spectral indices were extracted for the sampling points. Table 2 illustrates indices and the relations used for the calculation of these indices. The LAI index is based on ground-level measurements for mature pistachio trees in Yazd province and its calibration with Landsat TM has driven the SAVI index (Mokhtari et al., 2013).

Partial least square regression (PLSR) method was used to derive a relationship (model) between average measured soil salinity data at the representative points and the remotely sensed data. The PLSR is one of the classical and most commonly used multiple regression models (Guo et al., 2017), which provides the opportunity for simultaneous handling of multiple independent variables (e.g. satellite driven data bands and indices), which are expected to explain variability of the dependent variable (e.g. soil salinity). In this case study, the “leave one out” method of PLSR was used to find the preferred model(s).

3. Results and Discussion

3.1. Ground-based soil salinity predictions

In 12 out of 18 points, the WFD device could gather drain water, in which the salinity of the drainage water was measured. Table 3 shows the calculation of soil salinity based on the salinity of drain water in these 12 points. LF is calculated from the EC_{iw}/EC_{dw} ratio for each point. Knowing the LF, the concentration factor (X) is calculated from FAO 29 (Ayers and Westcot, 1985).

Table 3. The calculation procedures of estimated mean soil salinity based on drainage water salinity for the 12 points. The LF is calculated from the EC_{iw}/EC_{dw} ratio for each point.

Points	EC_{iw}	EC_{dw}	LF	X	EC_e (Eq. 3)	EC_e (WatSuit)	EC_e (measured)
P1	3.9	16.8	0.2	3.7	14.5	4.1	5.6
P2	4.0	28.7	0.1	5.1	20.2	5.4	9.1
P3	4.1	12.6	0.3	3.0	12.4	3.6	4.5
P4	3.8	17.8	0.2	3.9	14.8	4.0	4.0
P6	10.5	16.2	0.6	2.0	20.8	6.9	5.3
P7	10.1	28.8	0.3	2.9	29.0	9.0	9.2
P8	9.7	29.2	0.3	3.0	28.8	8.6	7.7
P11	14.4	34.1	0.4	2.6	37.0	11.6	14.1
P12	14.3	20.7	0.7	1.9	27.2	9.9	11.5
P15	19.1	53.7	0.4	2.8	54.5	16.1	13.5
P16	16.5	32.8	0.5	2.3	38.1	11.9	16.3
P17	11.1	37.0	0.3	3.2	35.2	10.4	14.7
Average	10.1	27.4	0.4	3.0	27.7	8.5	9.6

Table 4. Correlation matrix* between independent variables

	Band1	Band2	Band3	Band4	Band5	Band6	Band7	DEM	SAVI	NDVI	NDSI	NBRI	BSI
Band2	0.99												
Band3	0.96	0.98											
Band4	0.96	0.98	1.00										
Band5	0.15	0.25	0.34	0.34									
Band6	0.94	0.94	0.94	0.95	0.36								
Band7	0.95	0.93	0.94	0.94	0.17	0.96							
DEM	0.63	0.69	0.75	0.75	0.71	0.76	0.65						
SAVI	-0.98	-0.98	-0.97	-0.97	-0.13	-0.92	-0.95	-0.62					
NDVI	-0.98	-0.98	-0.97	-0.97	-0.13	-0.92	-0.95	-0.62	1.00				
NDSI	0.27	0.33	0.38	0.35	0.03	0.06	0.15	0.12	-0.38	-0.38			
NBRI	-0.93	-0.89	-0.88	-0.87	0.04	-0.90	-0.97	-0.51	0.93	0.93	-0.15		
BSI	0.96	0.95	0.94	0.94	0.13	0.96	0.98	0.64	-0.97	-0.97	0.16	-0.97	
LAI	-0.95	-0.96	-0.95	-0.94	-0.15	-0.89	-0.91	-0.62	0.98	0.98	-0.41	0.91	-0.96

*- values above ± 0.3 hcontributionally meaningful contributions in prediction of variables

Mean soil salinity (EC_e) was then calculated from Equation (3) by multiplying X by EC_{iw} .

The calculated LF (Table 3) was also used as an input parameter in the WatSuit model to predict mean soil salinity (EC_e (WatSuit)).

The last column in Table 4 presents the laboratory-measured mean soil salinity for comparison. Based on this table, the EC_e values calculated from the concentration factor (EC_e (Eq. 3)) are much higher than those predicted by the WatSuit and actual measurements. This means that at any specified LF, soil salinity predicted from (Eq. 3) is much higher than the value predicted from the WatSuit model, or to decrease the soil

salinity to a specified value, the (Ayers and Westcot, 1985) method predicts much higher leaching requirement in comparison to the WatSuit.

Figure 3 illustrates the linear regression between measured and predicted mean soil salinity by the WatSuit and the concentration factor (X). WatSuit predictions are much closer to 1:1 line and actual measurements.

Watsuit model is able to simulate the changes in major inorganic ions chemistry under different leaching fractions (Visconti et al., 2012). These changes could happen due to the precipitation and/or dissolution of carbonates in calcareous soils (De et al., 2017) depending on the leaching fraction and the concentration of ions.

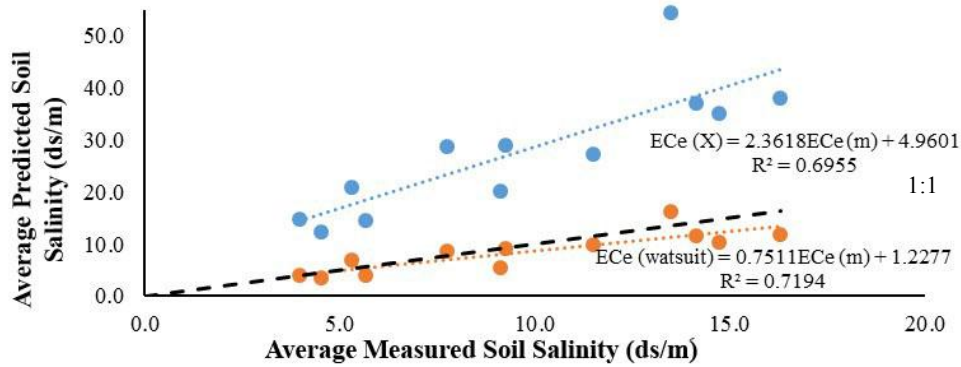


Fig. 3. Correlation between the measured ($EC_e(m)$) and predicted ($EC_e(Watsuit)$) mean soil salinity by WatSUIT and concentration factor (X)

Table 5. The coefficients of variables and ANOVA for the PLSR driven model to predict mean soil salinity

Variable	Coefficients		Analysis of Variance					
	ECe_avg	ECe_avg standardized	Source	DF	SS	MS	F	P
Constant	-99.0554	0.000000	Regression	2	284.380	142.190	13.44	0.000
band1	0.0006	0.027485	Residual Error	15	158.729	10.582		
band2	0.0015	0.071126	Total	17	443.109			
band3	0.0015	0.083975						
band4	0.0011	0.099141						
band5	0.0099	0.381828						
band6	0.0006	0.058744						
band7	-0.0001	-0.015001						
DEM	0.0653	0.366141						
savi	0.5111	0.015551						
ndvi	0.7665	0.015548						
NDSI	5.3891	0.033012						
NBRI	5.1140	0.113383						
BSI	-3.6525	-0.052738						
LAI	0.0838	0.047501						

The predicted soil salinity –considering the precipitation reactions by Watsuit model– could be lower than the values predicted just based on the concentration factor (X) which in turn, reduces the leaching requirement.

3.2. Satellite-based soil salinity prediction results

Table 4 shows the correlation matrix between independent variables used in this study (satellite driven data bands and indices). These variables may also be correlated to each other, which could hinder the multiple regression methods due to multicollinearity (Graham, 2003). The autocorrelation or collinearity tends to inflate the variance of estimated regression coefficients. To tackle the problem and predict soil properties from spectral data, the PLSR and the “leave one out” methods

were used, as well, to derive a preferred model (equation) between remotely sensed data and the measured mean soil salinity of the representative points.

Table 5 illustrates the coefficients of the preferred model and the Analysis of Variance (ANOVA) for the model obtained based on the Landsat 8 image on the soil sampling date (August 18th, 2019). Based on this table, there are strong correlations between these variables and soil salinity (significant at 0.0001 level) at the study area. Figure 4 shows the relationship between the measured and predicted soil salinities in comparison with the 1:1 line. Based on the results, the predictions are fairly correlated to the measurements. While the predicted salinities are generally overestimated in lower soil salinities and underestimated at higher soil salinities, they are close to the 1:1 line.

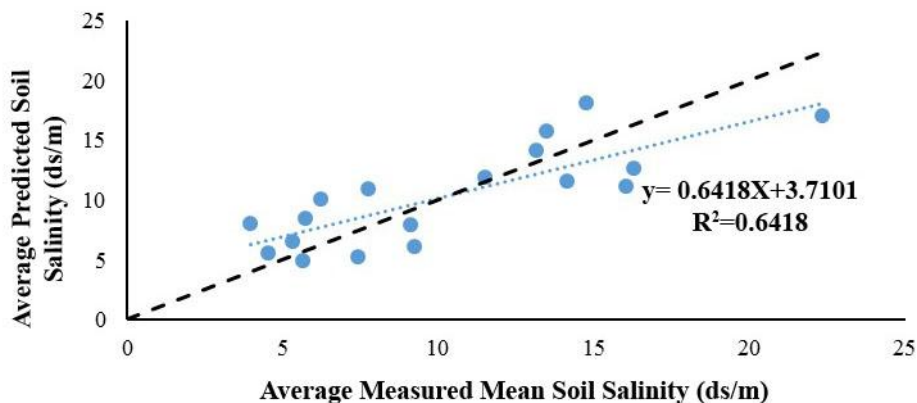


Fig. 4. The correlation between measured and predicted mean soil salinity by PLSR method

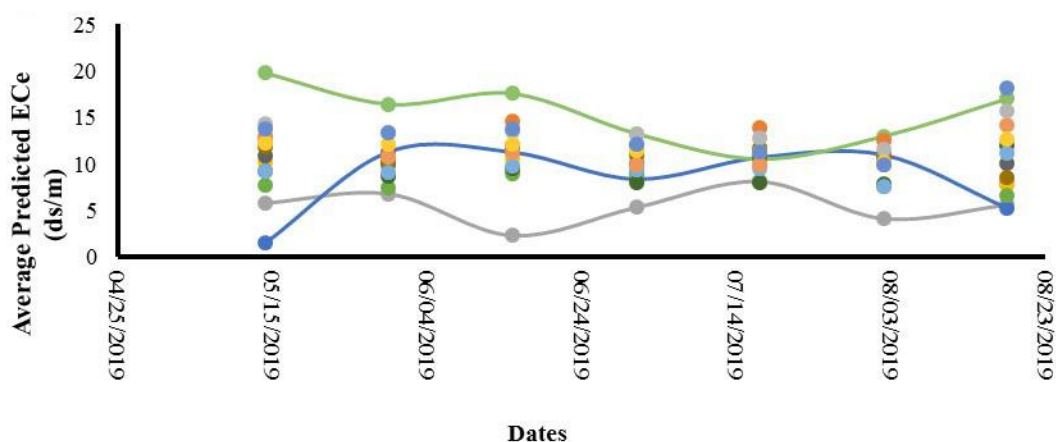


Fig. 5. The periodical pattern of soil salinity changes over time in the growing season. Dots are 18 sampling points and lines show the temporal changes of the predicted soil salinity for 3 points as examples.

The capability of Landsat 8 driven auxiliary data in predicting and mapping soil salinization was also reported by several authors among whom are Al-Khakani et al., (2018) for An-Najaf area in Iraq and Sahbeni (2021) in Great Hungarian Plain.

The coefficients of Table 5 were used to predict mean soil salinities at other dates during 2019 growing season, when the cloud-free Landsat 8 images were available (Fig. 5). The results of the simulation with this PLSR model showed a somewhat cyclic variability in the predicted soil salinities. The common schedule of irrigation in the area has 48 days of interval between the two subsequent irrigation events; as a result, soil moisture and soil solution salinity have a periodical pattern of variations between irrigations. The lowest soil salinity and the highest soil moisture occur exactly after irrigations. Regarding the irrigation schedule of the area, the interval between the two maximum or minimum values of soil salinity is expected to be about 48 days. As illustrated in Fig. 5, some points in the studied orchards show this trend sharply. The mentioned figure also shows a cyclic trend of soil salinity changes with time.

Monitoring of temporal variability in soil salinity is important in managing the leaching and irrigation of irrigated soils. Satellite-driven data are promising tools in prediction of these temporal variability. The landsat 5 TM and landsat 8 derived indices were used for monitoring of the soil salinity variability in Tuz (salt) lake area of Turkey in 1999 to 2015 period of time (Gorji et al., 2015). In the global scale, a similar approach is also applied to simulate the global changes in soil salinization (Hassani et al., 2020).

4. Conclusion

Both conventional and introduced approaches had the capability of simulating secondary soil salinization in the irrigated pistachio orchards of the Ardakan region, Central Iran. In comparison to WatSuit and the concentration factor (X) of conventional methods (Ayers and Westcot 1985), the WatSuit predictions were much closer to the actual measurements. This could be due to the capability of the WatSuit in considering the mineral dissolution of some carbonate species in calcareous soils

(Visconti et al., 2012). In the same leaching fraction, the concentration factor-based method predicted much higher mean soil salinity compared to the WatSuit method.

The introduced satellite-based approach was the most successful one in the prediction of salinity in the uppermost soil layers (Oster and Rhoades, 1990), while using the spectral indices which are correlated to the crop performance (e.g. SAVI and NDVI), the introduced PLSR model was able to estimate the mean root zone salinity with R^2 of 0.64.

The model was also able to predict the spatiotemporal variations of mean soil salinity. The temporal trend of soil salinity changes showed a periodical trend with intervals of 48 days, which was similar to irrigation intervals in the area. Also, the introduced model has the advantage of being independent of the ground truth data in comparison to traditional methods (e.g. WatSuit), while they need to be verified before out-scaling.

References

- Alexandre, C., Borralho, T., & Durão, A. (2018). Evaluation of salinization and sodification in irrigated areas with limited soil data, Case study in southern Portugal. *Spanish Journal of Soil Science*, 8, 102-120.
- AL-Khakani, E. T., Al-Janabi, W. F., & Sa'ad, R. Y., (2018). Using Landsat 8 OLI data to predict and mapping soil salinity for part of An-Najaf governorate. *Ecological Environmental Conservation*, 24, 572-578.
- Ayers, R., & Westcot, D. (1985). Water quality for agriculture. *FAO Irrigation and drainage paper 1*, vol 1. Food and Agricultural Organization. Rome.
- Baghzouz, M., Devitt, D., & Morris, R. (2006). Evaluating temporal variability in the spectral reflectance response of annual ryegrass to changes in nitrogen applications and leaching fractions. *International Journal of Remote Sensing*, 27(19), 4137-4157.
- Cheraghi, S., Hasheminejad, Y., & Heydari, N. (2008). Causes and management of salt-prone land degradation in lower Karkheh River Basin. Improving On-farm Agricultural Water Productivity in the Karkheh River Basin (CPWF Project no. 8). Research Report no. 1: *A Compendium of Review Papers*, Edited by: T. Oweis, H. Farhani, M. Qadir, J. Anthofer, H. Siadat, F. Abbasi and A. Bruggeman. ICARDA-AREO), 81-91.
- Cheraghi, S., Hasheminejad, Y., & Rahimian, M. (2007). An overview of the salinity problem in Iran: assessment and monitoring technology. Paper presented at the Advances in the assessment and monitoring of salinization and status of biosaline agriculture. Reports of expert consultation, Dubai, UAE.
- Corwin, D. L., & Grattan, S. R. (2018). Are existing irrigation salinity leaching requirement guidelines overly conservative or obsolete?. *Journal of Irrigation and Drainage Engineering*, 144(8), 02518001.
- Corwin, D. L., Rhoades, J. D., & Šimůnek, J. (2007). Leaching requirement for soil salinity control: Steady-state versus transient models. *Agricultural Water Management*, 90(3), 165-180.
- de Soto, I. S., Virto, I., Barré, P., Fernández-Ugalde, O., Antón, R., Martínez, I., Chaduteau, C., Enrique, A., & Bescansa, P. (2017). A model for field-based evidences of the impact of irrigation on carbonates in the tilled layer of semi-arid Mediterranean soils. *Geoderma*, 297, 48-60.
- Ghassemi, F., Jakeman, A. J., & Nix, H. A. (1995). Salinisation of land and water resources: human causes, extent, management and case studies. CAB international.
- Gorji, T., Tanik, A., & Sertel, E., (2015). Soil salinity prediction, monitoring and mapping using modern technologies. *Procedia Earth and Planetary Science*, 15, 507-512.
- Graham, M. H. (2003). Confronting multicollinearity in ecological multiple regression. *Ecology*, 84(11), 2809-2815.
- Guo, L., Zhao, C., Zhang, H., Chen, Y., Linderman, M., Zhang, Q., & Liu, Y. (2017). Comparisons of spatial and non-spatial models for predicting soil carbon content based on visible and near-infrared spectral technology. *Geoderma*, 285, 280-292.
- Hasheminejad, Y. (2011). Irrigation management under saline conditions using wetting front detector (WFD). *Iranian Journal of Soil Research (Formerly Soil and Water Sciences)*, 24(3), 265-272.
- Hasheminejad, Y., Cheraghi, A.M., Abbasi, A., Gholami, H., & Golshan, M. (2008). Investigation of the fate of salt below the root zone of irrigated lands in the north of Yazd-Ardakan plain. <https://civilica.com/doc/1096162>.
- Hasheminejad, Y., Gholami, M., & Soltani, V. (2012). Valuation of WatSuit model for prediction of alfalfa's root zone salt distribution pattern. *Iranian Journal of Water Research in Agriculture*, 26, 225-234.
- Hassani, A., Azapagic, A., & Shokri, N., (2020). Predicting long-term dynamics of soil salinity and sodicity on a global scale. *Proceedings of the National Academy of Sciences*, 117(52), 33017-33027.
- Ivushkin, K., Bartholomeus, H., Bregt, A. K., Pulatov, A., Kempen, B., & De Sousa, L. (2019). Global mapping of soil salinity change. *Remote Sensing of Environment*, 231, 111260.
- Jin, Y., He, R., Marino, G., Whiting, M., & Kent, E., (2018). Spatially variable evapotranspiration over salt affected pistachio orchards analyzed with satellite remote sensing estimates. *Agricultural and Forest Meteorology*, 262, 178-191.
- Mandal, A. (2019). Modern technologies for diagnosis

- and prognosis of salt-affected soils and poor-quality waters. In J. C., Dagar, R. K., Yadav, & P. C., Sharma (Eds.), *Research Developments in Saline Agriculture* (pp. 95-152). Springer Nature, Singapore.
- Manzoor, M.Z., Sarwar, G., & Aftab, M. (2019). Role of leaching fraction to mitigate adverse effects of saline water on soil properties. *Journal of Agricultural Research*, 57(4), 275-280.
- Metternicht, G., & Zinck, J. (2003). Remote sensing of soil salinity: potentials and constraints. *Remote Sensing of Environment*, 85(1), 1-20.
- Minasny, B., & McBratney, A. B. (2006). A conditioned Latin hypercube method for sampling in the presence of ancillary information. *Computers and Geosciences*, 32(9), 1378-1388.
- Minhas, P. S., Ramos, T. B., Gal, A. B., & Pereira, L. S. (2020). Coping with salinity in irrigated agriculture: Crop evapotranspiration and water management issues. *Agricultural Water Management*, 227, 105832.
- Moharana, P., Singh, R., Singh, S., Tailor, B., Jena, R., & Meena, M. (2019). Development of secondary salinity and salt migration in the irrigated landscape of hot arid India. *Environmental Earth Sciences*, 78 (15), 454.
- Mokhtari, M. H., Adnan, R., & Busu, I. (2013). A new approach for developing comprehensive agricultural drought index using satellite-derived biophysical parameters and factor analysis method. *Natural Hazards*, 65(3), 1249-1274.
- Noroozi, A. A., Homaei, M., & Abbasi, F. (2012). Integrated application of remote sensing and spatial statistical models to the identification of soil salinity: a case study from Garmsar plain, Iran. *Environmental Sciences*, 9, 59-74.
- Oster, J. D., & Rhoades, J. D. (1990). Steady State Root Zone Salt Balance. In K. K. Tanji, (ed.) *Agricultural Salinity Assessment and Management Manual. ASCE Manuals and Reports on Engineering Practice No. 71* (pp. 469-481). American Society of Civil Engineers.
- Qadir, M., Quill rou, E., Nangia, V., Murtaza, G., Singh, M., Thomas, R.J., Drechsel, P., & Noble, A. D. (2014). Economics of salt-induced land degradation and restoration. *Natural Resources Forum* (4), 282-295.
- Qadir, M., Qureshi, A.S., & Cheraghi, S. (2008). Extent and characterization of salt-affected soils in Iran and strategies for their amelioration and management. *Land Degradation and Development*, 19(2), 214-227.
- Rahimian, M.H., Shayannejad, M., Eslamian, S., & Gheysari, M. (2019). Daily and seasonal pistachio evapotranspiration in saline condition: comparison of satellite-based and ground-based results. *Journal of the Indian Society of Remote Sensing*, 47(5), 777-787.
- Rhoades, J., Kandiah, A., & Mashali, A. (1992). The use of saline waters for crop production. *FAO Irrigation and Drainage Paper*, 133(48).
- Sahbeni, G., (2021). Soil salinity mapping using Landsat 8 OLI data and regression modeling in the Great Hungarian Plain. *SN Applied Sciences*, 3(5), 1-13.
- Stirzaker, R. (2005). Managing irrigation with a wetting front detector. *UK IRRIGATION*, 33:22.
- Stirzaker, R. J. (2003). When to turn the water off: Scheduling micro-irrigation with a wetting front detector. *Irrigation Science*, 22, 177-185.
- Vermote, E., Justic, C., Claverie, M., & Belen, F. (2016). Preliminary analysis of the performance of the Landsat 8/OLI land surface reflectance product. *Remote Sensing of Environment*, 185, 46-56.
- Visconti, F., Paz, J. M. D., Rubio, J., & S nchez, J. (2012). Comparison of four steady-state models of increasing complexity for assessing the leaching requirement in agricultural salt-threatened soils. *Spanish Journal of Agricultural Research*, 10(1), 222-237.
- Welle, P. D., & Mauter, M. S. (2017). High-resolution model for estimating the economic and policy implications of agricultural soil salinization in California. *Environmental Research Letters*, 12(9), 094010.
- Yang, T., Šim nek, J., Mo, M., McCullough-Sanden, B., Shahrokhnia, H., Cherchian, S., & Wu, L. (2019). Assessing salinity leaching efficiency in three soils by the HYDRUS-1D and -2D simulations. *Soil and Tillage Research*, 194, 104342.